POAC'17
Busan, KOREA

Proceedings of the 24th International Conference on
Port and Ocean Engineering under Arctic Conditions
June 11-16, 2017, Busan, Korea

Relation of Maximum Structural Velocity and Ice Drift Speed during Frequency Lock-In

Gesa Ziemer[1], Philipp Hinse[1]
[1] HSVA, Hamburg, Germany

ABSTRACT

Ice model tests with compliant cylindrical structures have been conducted at the Hamburg Ship Model Basin. Ice-induced frequency lock-in vibrations have been observed at different ice drift speeds without variation of other ice parameters. Adapting to different ice drift speeds while vibrating in a frequency close to its natural frequency is possible for the structure mainly due to a variation of the ratio β of maximum structural velocity (V_A) and ice drift speed (U). The paper describes the test setup and main observations from the model test campaign. Boundaries of β are derived based on the model test observations and compared to literature. A formula is presented to estimate the transitional velocities to the possible lock-in range based on β-variation. It is possible to predict the complete range of critical velocities for a given structural configuration based on only one observed lock-in event. A comparison of calculations and measurements shows promising results.

KEY WORDS: Frequency lock-in; Model tests in ice; Ice-induced Vibrations

INTRODUCTION

Ice-induced frequency lock-in vibrations have been subject to extensive research since the late 1960s. Soon after the first observations of lock-in vibrations in full scale, two different mechanisms have been proposed to explain the violent oscillations: Peyton (1968) claims that a characteristic failure length exists, which can correspond to the natural frequency of the structure at certain ice drift speeds and thereby creates a resonant condition. Blenkarn (1970) was the first to propose that lock-in is the result of some source of negative damping. Both concepts have been further developed and most of today's theoretical and numerical models are based on one of them. Despite all research efforts, both explanations are still under debate, and none of the currently existing models is able to predict the occurrence of lock-in with satisfying accuracy (Kärnä et al., 2013). Current research partly concentrates on the role of contact area and high pressure zones, employing rather new measuring techniques that provide better insight into local phenomena (e.g. Ziemer and Deutsch, 2015; O'Rourke et al., 2016; Hendrikse and Metrikine, 2017).

The IVOS project follows this trend and aims at studying the contact area and behavior of high pressure zones during different types of dynamic ice-structure interaction to gain more insight into the physical mechanism leading to lock-in. As a first step, model tests have been performed to create a broad basis for theoretical considerations and model validation. These tests are used in the presented study to formulate a relation of critical ice drift velocities that

may lead to lock-in vibrations based on known structural parameters. Note that no scaling was applied, thus all presented results are valid for model scale regime only.

MODEL TESTS

Model tests in ice with compliant cylindrical single-degree of freedom (SDOF) structures have been performed as part of the IVOS project in HSVA's Large Ice Basin in 2015 and 2016. The physical tests were divided into two phases: Phase 1 with a bottom-fixed cylindrical structure, using active loading (structure at rest and moving ice sheet), and Phase 2 with cylindrical and flat structures employing passive loading (structure is pushed through resting ice sheet). Main objectives of the two test series were:

- Development and check of a physical test setup to conduct experiments on ice-induced vibrations with a variety of structures
- Data collection of local ice load measurements to gain insight into dynamic ice-structure interaction and corresponding pressure distribution as well as failure processes

The two test phases are briefly described below.

Phase 1

A compliant basis mounted to the basin's floor was used for Phase 1 tests. The setup bases on previous model test campaigns (see Onken et al. (2013), Ziemer and Evers (2016)) and had been optimized in several steps. The latest version is described by Ziemer and Deutsch (2016) and presented in Figure 1 (left). The compliant basis (yellow) is fixed to a rigid frame (green) by coil springs and linear bearings. A cylindrical model (red) with 830mm diameter was used for the tests. This model was equipped with tactile sensors to monitor local ice loads. Additionally, global loads were recorded by a 6-component load scale connecting the compliant basis and the model, and lasers and accelerometers monitored the ice-induced vibrations of the structure in x- and y-direction (loading direction and perpendicular in-plane motion).

Test conditions are summarized in Table 1. Prior to the tests, the level ice sheet was cut loose from the side walls of the basin. A 10m long stripe of ice was pushed against the structure during each test run by the main carriage. Different failure modes have been observed throughout the test campaign, covering the regimes of intermittent crushing, lock-in and continuous crushing. Due to the relatively high elasticity of the model ice, the ice tended to bend downwards before crushing against the structure. Therefore, the interaction was interrupted frequently by bending failure. This behavior is amplified by the structure's large aspect ratio. At times, release cracks formed that ran from the pushing board of the main carriage towards the structure or the side walls of the basin. Another downside of this setup is the location of the springs at the submerged compliant basis, making all changes of stiffness and natural frequency time consuming. Also, the huge compliant basis built as a steel framework adds considerable hydrodynamic mass and damping.

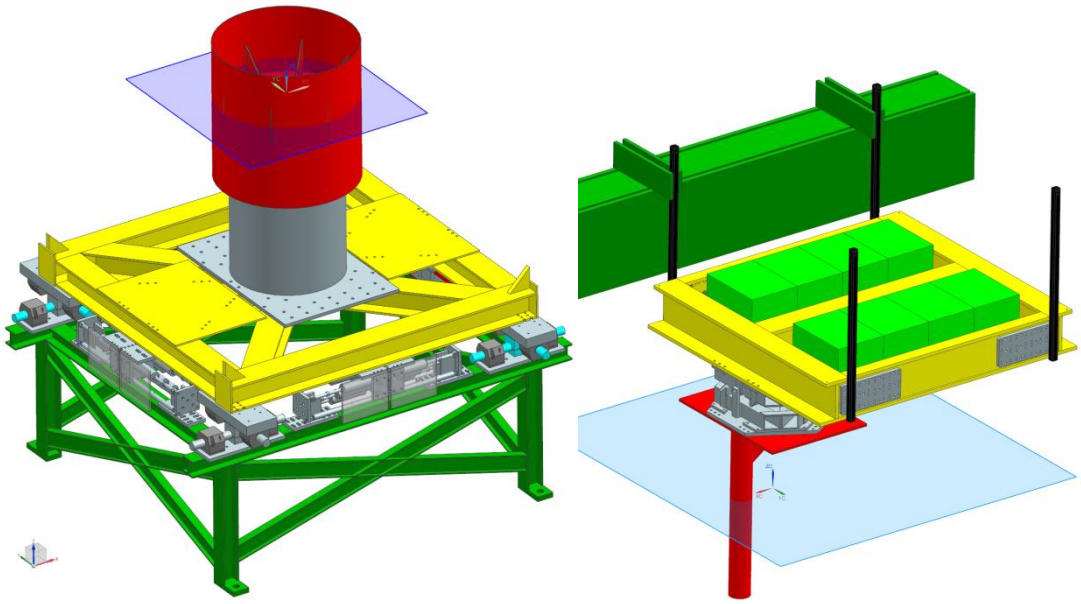

Figure 1. Left: Drawing of the setup used for Phase 1 tests (active loading, mounted to the basin's floor). Right: Drawing of Phase 2 setup (passive loading, mounted to the main carriage)

Table 1. Test conditions Phase 1 (mean values).

Series	Cylinder diameter [mm]	Natural frequency [Hz]	Stiffness [N/mm]	Ice thickness [mm]	Compressive strength [kPa]	Tested ice drift velocity range [m/s]
11000	830	5.5	2230	50	72	0.010 – 0.15
12000	830	5.5	2230	48	95	0.005 – 0.06
13000	830	2.7	490	46	79	0.020 – 0.15
14000	830	2.7	490	46	114	0.010 – 0.044

Phase 2

A new setup was designed for Phase 2 to be more flexible with changes of the model. Passive loading was utilized by attaching a compliant basis to the rigid moonpool of the main carriage, which holds the model and provides the aspired dynamic properties. Aluminum rods with box sections are used as flexible springs. The top mass on the compliant platform can be varied to adjust the natural frequency. The setup is shown in Figure 1 (right).

Passive loading means that the ice sheet can remain frozen to the side walls of the basin. Thus, release cracks are far more unlikely than with passive loading. The acceleration of the main carriage was monitored to check whether control oscillations are transferred to the model. This was not the case; the soft springs are an effective damper for the high frequency oscillations of the main carriage. Shape and diameter of the models were varied: Cylinders were tested with diameters of 120mm, 200mm and 500mm, and a flat indenter with rectangular cross section and width of 200mm was tested additionally in side-first and corner-first configuration. Only results from cylindrical models are considered in this paper. Similar to Phase 1, all models were equipped with tactile sensors and the global loads were measured by a 6-component scale. Lasers and accelerometers monitored the in-plane vibratory motion of the models. The smaller aspect ratios limited the bending failure of the ice sheet at the

structure. This occurred only on some of the structures in a certain velocity range. By varying the carriage speed in small steps of 1 mm/s, the transition from intermittent crushing to steady-state response and later to continuous crushing was captured well for all tested structures.

Relevant test conditions studied in Phase 2 are summarized in Table 2.

Table 2. Test conditions Phase 2 (mean values).

Series	Cylinder diameter [mm]	Natural frequency [Hz]	Stiffness [N/mm]	Ice thickness [mm]	Compressive Strength [kPa]	Tested ice drift velocity range [m/s]
21000	500	5.5	2220	31	90	0.005 – 0.10
21000	500	7.6	3020	31	80	0.005 – 0.10
23000	200	5.8	1930	33	82	0.005 – 0.15
23000	200	5.8	1930	42	97	0.005 – 0.15
23000	500	5.5	2030	43	72	0.005 – 0.10
24000	120	5.4	1935	41	136	0.005 – 0.20

RESULTS

The main objective of the tests was to create data sets which cover a large range of ice drift speeds to monitor the transitional velocities limiting the interval where frequency lock-in occurs. A comparison of the conditions leading to lock-in of different structures and in different ice conditions can shed some light onto the still unresolved question of how frequency lock-in develops.

Lock-in has been observed with all tested structural configurations. In most tests, lock-in was monitored along with intermittent and continuous crushing within the same test run, thus without changes of ice parameters except for the simulated ice drift speed. An example of lock-in is given in Figure 2, showing the almost purely sinusoidal response close to the structure's natural frequency, and periodic ice load. Lock-in events had a duration between 7s and 60s.

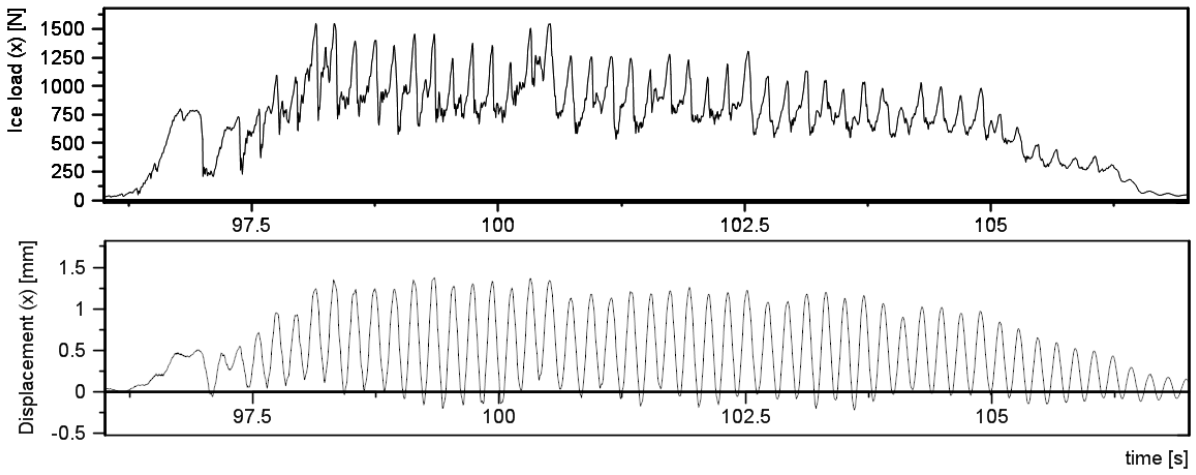

Figure 2. Example of frequency lock-in vibrations observed during Run 12050.

Characterization of a Lock-in Cycle

All time series obtained in the IVOS test phases containing frequency lock-in vibrations show a characteristic time history of load and corresponding response during each loading cycle, which is presented in Figure 3. While a lock-in cycle is often subdivided into a *loading phase* and an *unloading phase* in common literature (compare e.g. ISO 19906:2010), the test results indicate that a further subdivision of the loading phase into a *crushing phase* and a *build-up phase* is reasonable. The unloading phase is referred to as *collapse phase* within this study.

The cycle starts at position ①: After the ice has collapsed in the previous cycle, the deflected structure is released and starts to move back to its equilibrium position. Herein, the equilibrium refers to the mean deflection around which the structure oscillates. When this position is reached, the relative velocity between structure and ice is at its maximum, as structure and ice move in opposite direction. The structure starts to penetrate into the ice and crushes it, which decelerates the structural movement and eventually turns the orientation of movement: When the stored energy is not sufficient to crush the ice any longer, the ice deflects the structure instead. Thus, the relative velocity decreases to almost zero at position ②. This is the case after about one half natural period, and the structure is again close to its equilibrium position at this point in time. This is when the *build-up phase* starts: the ice load increases significantly and deflects the structure while the relative velocity increases as well. When the maximum of deflection is reached (③) the ice fails, and the collapse phase starts. During collapse, the structure is released and returns to its initial position. Then the cycle starts anew.

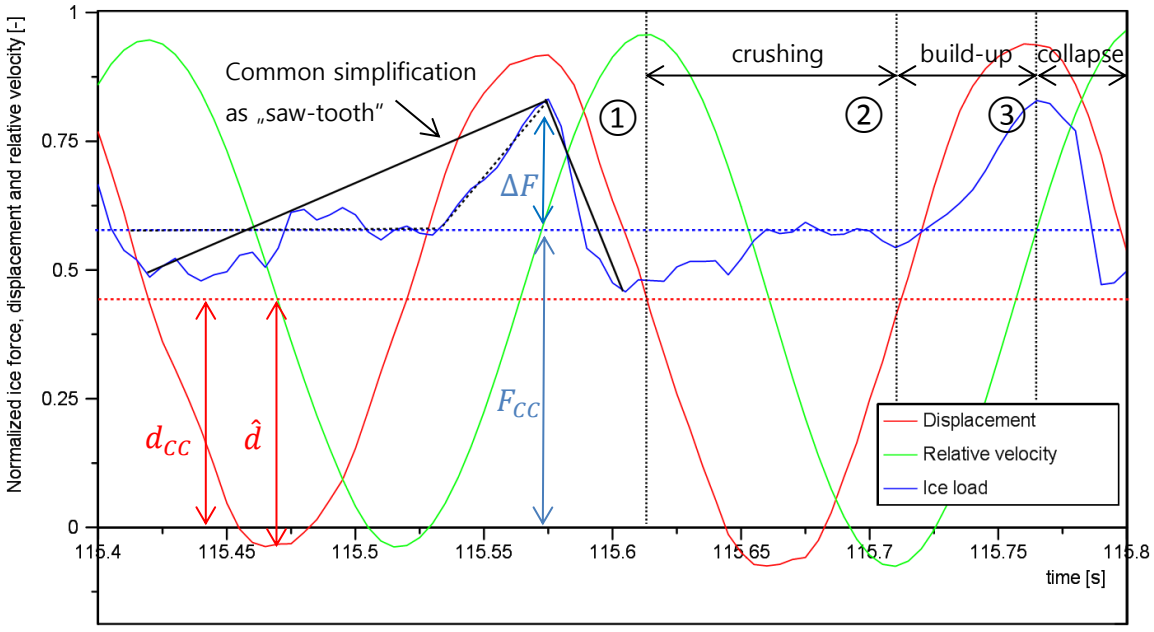

Figure 3. Phases of a lock-in cycle as observed in IVOS tests.

Calculation of Critical Velocities

It is currently not possible to predict critical velocities for the occurrence of lock-in based on structural and ice parameters with reasonable accuracy, but small calculation efforts. The considerations presented in this section are a step towards such prediction formula.

The previous section has shown that a lock-in cycle has a certain characteristic, mainly prescribed by the initiation and termination of the *build-up phase*. The phase relation of load and response during build-up helps to describe the motion in a simplified way: For further considerations, we simplify the structural response as a purely sinusoidal oscillation which can be described by following function (compare Figure 3):

$$d(t) = d_{CC} + \hat{d}\sin(\omega t) \quad (1)$$

Herein, d_{CC} is the mean deflection at equilibrium position, thus the deflection resulting from the mean crushing force F_{CC} and the structural stiffness k:

$$d(t) = \frac{F_{CC}}{k} + \hat{d}\sin(\omega t) \quad (2)$$

With some simplification, we may define the ice load function as a combination of a time invariant mean crushing force F_{CC} and a time-dependent force $\Delta F(t)$ representing the load increase:

$$F_{ice}(t) = F_{CC} + \Delta F(t) \quad (3)$$

Such description is not correct for collapse and crushing phase, but with the sine function for displacement and a linear load increase during build-up, ice load and structural response are easy to describe for this specific phase of the lock-in cycle.

At position ③, $\Delta F(t)$ becomes ΔF (maximum), and relative velocity between ice and structure becomes almost zero. Hence, we can use the equation of motion to describe the relation of ice load, inertia load and spring force at point ③ which has to be fulfilled to meet a lock-in condition as found in the tests:

$$F_{CC} + \Delta F = -\omega^2 m\hat{d} + k\left(\frac{F_{CC}}{k} + \hat{d}\right) \quad (4)$$

Engelbrektson (1997) was the first to observe that lock-in vibrations occur when the ice drift speed is similar to the maximum velocity of the structure during vibrations, thus when the amplitude of the almost sinusoidal response velocity equals the mean ice drift speed. Subsequently, Kärnä et al. (2007) and others compiled evidence that a certain velocity ratio β between maximum structural velocity V_A and ice drift speed U is required for lock-in:

$$V_A = \beta U = \hat{d}\omega \Rightarrow \hat{d} = \frac{\beta U}{\omega} \quad (5)$$

Kärnä et al. (2007) state that β has to be in a range between 0.9 and 1.4. Inserting eq. (5) in (4) and solving for U yields a formulation for the critical ice drift velocities which allow for lock-in:

$$U = \frac{\omega \Delta F}{\beta(k - \omega^2 m)} \quad (6)$$

It should be noted that this relation of ice drift speed and structural parameters does not imply any physical explanation of lock-in, but rather provides necessary conditions that have to be met in order to maintain a frequency lock-in condition. Although eq. 6 contains several major simplifications, it can be a helpful tool to estimate critical velocities if the unknowns can be predicted in a reasonable range. These predictions are subject to the following sections.

Estimates for Oscillation Frequency ω

During frequency lock-in, the structure oscillates in a frequency close to its natural frequency. IVOS tests indicate a range of $\omega = 0.90 \ldots 0.99\, \omega_n$. This is slightly different from what Kärnä (1994) reported: He found the vibration frequency during lock-in to be 5-15% lower than the natural frequency of the structure ω_n. It should be noted that the vibration frequency can be assumed to be dependent on ice conditions and structural parameters rather than on ice drift speed, as ω is found to be almost constant for each test run (compare example shown in Figure 4).

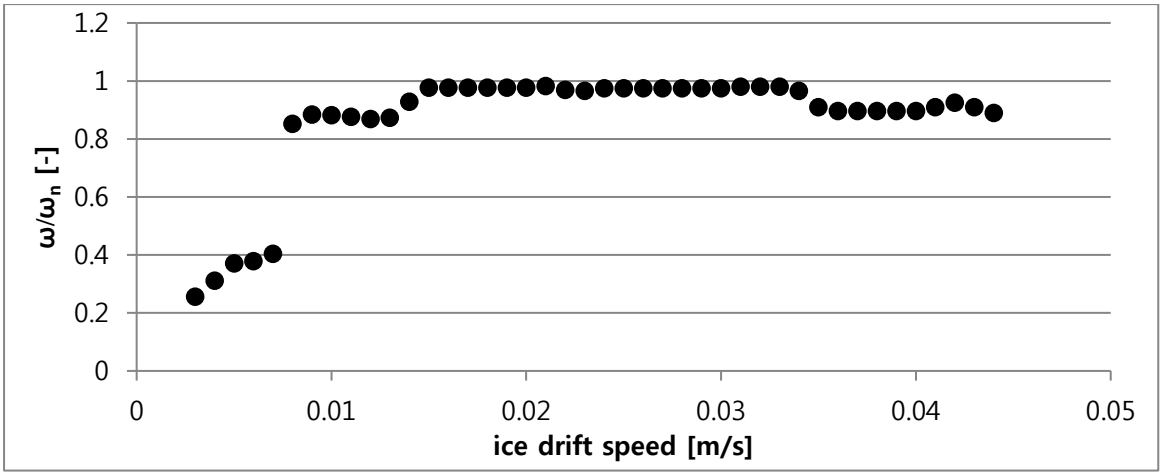

Figure 4. Trend of response frequency over simulated ice drift speed (all values taken from the same test run).

Prediction of ΔF

The increase of global load ΔF during build-up phase is one of the essential parameters to estimate the critical velocities for lock-in. It may depend on ice parameters (i.e. ice thickness, compressive strength) as well as on structural parameters (i.e. diameter of the cylinder, combination of stiffness and natural frequency). The variation of test conditions in the two phases of the IVOS project provides a good basis to study these influences. Such study is still on-going, but first findings are presented below.

Influence of ice parameters

Naturally, the crushing load level depends on the compressive strength of the model ice. Results from Phase 1 tests with invariant structural configurations and ice sheets with similar thickness, but varying strength, confirm a fairly linear increase of crushing load over increasing uniaxial compressive strength (Figure 5). Data indicates that ΔF increases linearly as well. Thus, the ratio of build-up force and mean crushing force remains the same, regardless of ice strength.

The ice thickness variation during the test campaign was too small to allow for significant conclusions about its influence on the build-up force. Detailed analysis of the local loads is

required to develop a theory about the influence of the ice thickness on the local pressure distribution which affects ΔF.

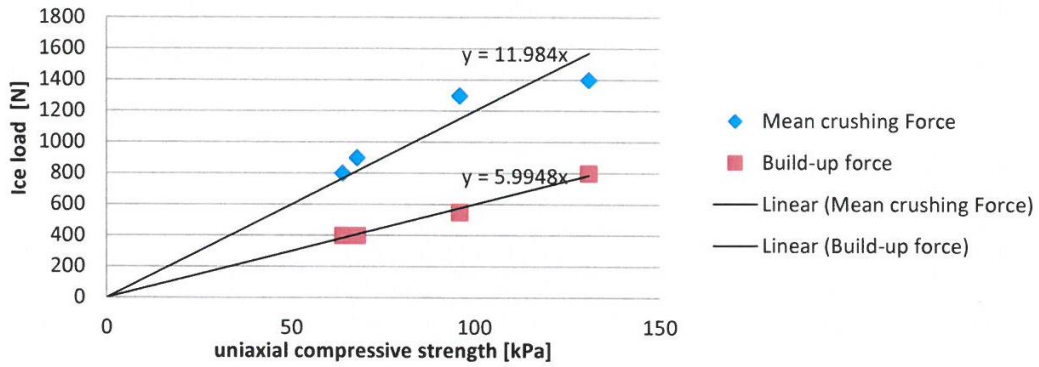

Figure 5. Trend of mean crushing force (F_{CC}) and average build-up force (ΔF) over uniaxial compressive strength of the model ice.

Influence of Structural Parameters

No significant difference between the build-up forces on structures with the same diameter, but varying dynamic properties (mass, stiffness, natural frequency) has been found in the tests. But the mean crushing load depends on the diameter of the tested cylinder, and so does the build-up force. Also, the ratio of build-up force and mean crushing force changes with changing cylinder diameter. Deciphering this relation is subject to current research.

Trend of Maximum Structural Velocity and Ice Drift Speed

Rearranging eq. 6 describes a relation of the build-up force and the inertial and spring forces acting on the structure:

$$\Delta F = -\beta(\omega^2 m + k)U \tag{8}$$

It has been shown above that the build-up force does not change with changing ice drift speed. Also, the term $\omega m + \frac{k}{\omega}$ is not dependent on U as illustrated in Figure 5. Therefore, the expression βU must be nearly constant (Toyama et al., 1983), and the ability of the structure to enter the lock-in condition at different ice drift speeds results from the variability of β. An example of the trend of β over ice drift speed is presented in Figure 6: At low speeds, β is high. As the ice drift speed increases the ratio β becomes smaller and approaches unity. When the ice drift speed increases further, the displacement amplitudes cannot increase accordingly, and β approaches zero.

Kärnä et al. (2007) found β to be in a range between 0.9 and 1.4 during lock-in for a collection of full scale and small scale data. Yap and Palmer (2013) limited this range to 0.9 to 1.1. Thus, the upper bound is somewhat uncertain.

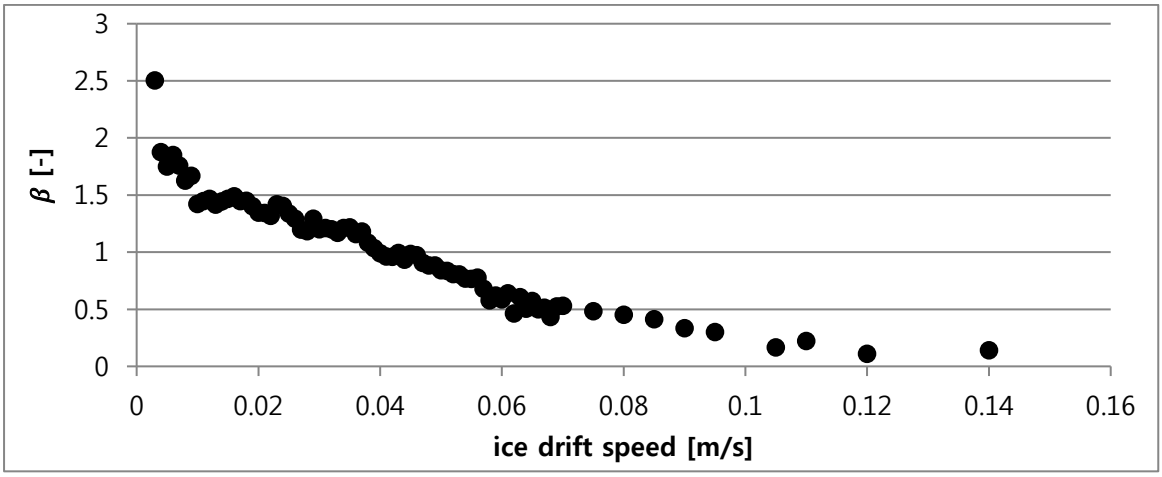

Figure 6. Trend of β over simulated ice drift speed (all values taken from the same test run).

We can find a physical upper limit for β by considering the displacement of the ice sheet during the build-up phase: While the ice edge travels a distance $\Delta d_{ice} = U\Delta t$ within a quarter period ($\Delta t = \frac{\pi}{2\omega}$), the structure deflects by $\hat{d} = \frac{\beta U}{\omega}$ (see eq. 5). We know from the local load measurements that ice and structure never lose contact during build-up phase – otherwise, the load increase would not be possible. Therefore, the displacement amplitude at highest possible β must be smaller than or equal to the distance travelled by the ice edge:

$$\frac{\beta_{max} U}{\omega} \geq U \frac{\pi}{2\omega} \Rightarrow \beta_{max} = \frac{\pi}{2} \tag{7}$$

Eq. 7 corresponds well to the maximum β found in literature. From eqs. 6 and 7 we obtain a formulation for the maximum ice drift speed at which lock-in is theoretically possible:

$$v_{II} = \frac{2\omega\Delta F}{\pi(k - \omega^2 m)}$$

The lower boundary for β depends on the maximum relative velocity at which the build-up phase can be initiated. The value of 0.9 from literature is taken as lower boundary for this study:

$$v_I = \frac{\omega\Delta F}{0.9(k - \omega^2 m)}$$

Comparison of Theoretical and Experimental Results

If the build-up force ΔF is known, critical velocities can be calculated using the derived boundaries for β, known structural parameters, and estimates for ω. At the moment it is not possible to estimate ΔF and ω with sufficient accuracy to use the formula for a prediction of critical conditions for lock-in without experimental results. But if one lock-in event has been monitored on a structure, we can use it to find other conditions which are critical as well. The easiest case is to assess the risk of lock-in based on variation of ice drift speed, but constant ice thickness and strength. This is done for all test runs from the IVOS campaign where lock-in has been observed at different simulated ice drift speeds. For each run, one

lock-in event was arbitrarily chosen as a base case. ΔF was calculated as the mean build-up force during the steady-state of the specific event, and ω was found by spectral analysis of its displacement time history. Boundaries for β were set to 0.9 and $\frac{\pi}{2}$. Results are presented in Table 3.

Table 3. Calculated and measured critical velocities for the occurrence of lock-in.

Run	**12050**	**13050**	**21020**	**23010**	**23020**	**24010**
Natural frequency f_n [Hz]	5.45	2.65	7.60	5.80	5.47	5.40
Oscillation frequency during lock-in f [Hz]	5.12	2.52	7.31	5.69	5.42	5.34
f/f_n	0.94	0.95	0.96	0.98	0.99	0.99
Stiffness k [N/m]	2230	490	3020	1930	2030	1935
Ratio of critical damping ξ [%]	1.5	3.0	2.7	2.3	3.1	2.3
Oscillating (modal) mass m [kg]	1712	1591	1192	1308	1547	1513
Average build-up force ΔF based on one arbitrarily chosen event with full ice contact [N]	481	273	264	249	251	131
v_I (calculated) [m/s]	0.021	0.030	0.015	0.022	0.023	0.012
v_I (measured) [m/s]	0.020	0.032	0.020	0.020	0.020	0.009
v_{II} (calculated) [m/s]	0.037	0.053	0.027	0.038	0.040	0.021
v_{II} (measured) [m/s]	0.040	0.050	0.030	0.040	n.a.	0.024

Note that the simulated ice drift speed was incrementally increased using steps of 0.001 m/s (Runs 13050 and 24010), 0.005 m/s (Run 21020) and 0.01 m/s (all other runs). Therefore, the transitional velocities have not been determined with higher accuracy than 0.01 m/s for most runs, and the above fit is satisfactory. In Run 23020, the failure mode changed to buckling instead of continuous crushing; therefore, no experimental upper transitional velocity can be provided.

Although the results show a very good fit, one has to be cautious because of several uncertainties that influence the critical velocities: We assume ice conditions to be homogeneous along the model basin, but in reality there is some variation in thickness and strength which affects the build-up force and the damping during lock-in. Also, the build-up force depends on the contact between structure and ice: After flexural failure, the new ice edge is often asymmetric, and the contact does not fully develop over the structure's circumference. Hence, the build-up force in this case differs from the full contact condition. Furthermore, evaluated events were arbitrarily chosen and only a steady-state part of it was used to determine the mean build-up force. Choosing a different event or a different interval leads to variations of ΔF and thus variation of calculated critical velocities.

SUMMARY AND CONCLUSIONS

Model tests in ice have been performed with a variety of structures as part of the IVOS project. Active and passive loading has been utilized for the test setups. Passive loading

seems to be the more reasonable choice for future tests because the setup allowed for more flexibility in changing the models and their structural parameters.

All tested structures were successfully set into lock-in vibrations and the global and local loads as well as the structural response have been measured for different types of ice-structure interaction. The load time histories revealed that the classic definition of a loading and unloading phase, creating a saw-tooth shaped forcing function, may be an oversimplification. This observation was the basis for a simple formula describing the relation of load increase and corresponding structural response during lock-in, mainly influenced by the relation of maximum structural velocity and ice drift speed (β). Although this formula cannot yet be used to predict the occurrence of lock-in for a specific structure without any experiments or full scale observations, it is useful to estimate the range of critical ice conditions based on only one lock-in event. A comparison of experimental and theoretical results shows promising agreement.

The topic of ice-induced lock-in vibrations remains a challenge. The IVOS test results form a valuable basis to shed some more light on unresolved questions. Especially the local load measurements can help to increase the understanding of the phenomenon. More research is needed to decipher the underlying physical mechanisms. Current research concentrates on data analysis with respect to contact area and the behavior of high pressure zones during the different phases of lock-in. This will also help to predict the build-up force theoretically.

ACKNOWLEDGEMENT

The tests have been conducted as part of the SAMCoT-associated project IVOS. Authors are grateful to the Research Council of Norway for the support of the Centre for Research-based Innovation SAMCoT and the support of all SAMCoT partners. In particular, authors wish to thank SAMCoT partners additionally involved in the IVOS project, contributing by valuable feedback and financial support: DNV GL, Engie SA, Kvaerner Concrete Solution AS, Multiconsult AS, Shell Technology Norway AS, Total E&P Norge AS, NTNU and TU Delft.

The authors are also grateful for the financial support of the data analysis by the German Federal Ministry for Economic Affairs and Energy (BMWi) through the project CoPSIS (O3SX408A).

REFERENCES

Blenkarn, K. A., 1970. Measurements and analysis of ice forces on Cook Inlet structures. In Proceedings of the Second Annual Offshore Technology Conference, volume II, pp 365–378, Houston, Texas.

Engelbrektson, A., 1997. A refined ice/structure interaction model based on observations in the Gulf of Bothnia. Proceedings of the Int. Conf. on Port and Ocean Engineering under Arctic Conditions (POAC). Yokohama, Japan, Vol. 4, pp. 373-376.

Hendrikse, H. & Metrikine, A., 2015. Interpretation and prediction of ice induced vibrations based on contact area variation. Int. J. Solids Struct., 75-76:336–348.

Kärnä, T., 1994. Steady-state vibrations of offshore structures. Hydrotechnical Construction, 28(8):446-453.

Kärnä, T., Izumiyama, K., Yue, Q., Qu, Y., Guo, F. & Xu, N., 2007. Ab upper bound model for self-excited vibrations. Proc. of the Int. Conf. on Port and Ocean Engineering under Arctic Conditions (POAC). Dalian, China, Vol. 1, pp. 177-189.

Kärnä, T., Andersen, H., Gürtner, A., Metrikine, A., Sodhi, D., Loo, M., Kuiper, G., Gibson, R., Fenz, D., Wallenburg, C., Wu, J.-F. & Jefferies, M., 2013. Proceedings of the 22nd International Conference on Port and Ocean Engineering under Arctic Conditions (POAC), Espoo, Finland.

Onken, G., Haase, A., Evers, K.-U. & Jochmann, P., 2013. Ice model tests with a cylindrical structure to investigate dynamic ice-structure interaction. Proceedings of the 22nd International Conference on Port and Ocean Engineering under Arctic Conditions (POAC), Espoo, Finland.

O'Rourke, B., Jordaan, I., Taylor, R. & Gürtner, A., 2016. Experimental investigation of oscillation of loads in ice high-pressure zones, part 1: Single indentor system. Cold regions science and technology 124 (2016) pp. 25-39.

Peyton, H. R., 1968. Sea ice forces. In Ice Pressures Against Structures, compiled by L. Gold and G.Williams, NRC Techn.Memo No. 92, Ottawa, Canada.

Toyama, Y., Sensu, T., Minami, M., & Yashima, N., 1983. Model tests on ice-induced self-excited vibration of cylindrical structures. In Proceedings of the Seventh International Conference on Port and Ocean Engineering under Arctic Conditions (POAC), vol 2, pp 834–844, Helsinki, Finland.

Yap, K.T. & Palmer, A., 2013. A model test on ice-induced vibrations: Structure response characteristics and scaling of the lock-in phenomenon. Proceedings of the 22nd International Conference on Port and Ocean Engineering under Arctic Conditions (POAC), Espoo, Finland.

Ziemer, G. & Deutsch, C., 2015. Study of local pressure distribution and synchronization during frequency lock-in. Proceedings of the 23rd International Conference on Port and Ocean Engineering under Arctic Conditions (POAC), Trondheim, Norway.

Ziemer, G. & Evers, K.-U., 2016. Model Tests with a Compliant Cylindrical Structure to Investigate Ice-Induced Vibrations. Journal of Offshore Mechanics and Arctic Engineering 138(4)